Journal of Magnetism and Magnetic Materials 324 (2012) 2205–2210

Contents lists available at SciVerse ScienceDirect

Journal of Magnetism and Magnetic Materials

journal homepage: www.elsevier.com/locate/jmmm

Effects of magnetic annealing on structure and multiferroic properties of pure and dysprosium substituted $BiFeO_3$

Shuxia Zhang [a,1], Yingbang Yao [b,1], Yao Chen [a], Dongliang Wang [a], Xianping Zhang [a], Satoshi Awaji [c], Kazuo Watanabe [c], Yanwei Ma [a,*]

[a] Institute of Electrical Engineering, Chinese Academy of Sciences, P.O. Box 2703, Beijing 100190, China
[b] Imaging and Characterization Core Laboratory, King Abdullah University of Science and Technology, Thuwal 23955-6900, Saudi Arabia
[c] High Field Laboratory for Superconducting Materials, Institute for Materials Research, Tohoku University, Sendai 980-8577, Japan

ARTICLE INFO

Article history:
Received 15 June 2011
Received in revised form
13 December 2011
Available online 25 February 2012

Keywords:
Multiferroic material
Magnetic annealing
Ferromagnetism
Ferroelectric property

ABSTRACT

In this work, the effects of magnetic annealing on crystal structure and multiferroic properties of $BiFeO_3$ and $Bi_{0.85}Dy_{0.15}FeO_3$ have been investigated. It is found that the X-ray diffraction patterns of pure $BiFeO_3$ samples are obviously broadened after magnetic annealing, whereas those of $Bi_{0.85}Dy_{0.15}FeO_3$ samples are almost unchanged. Magnetic field annealing did not affect the magnetic properties of these two kinds of samples much. However, ferroelectric properties of the two materials exhibited different behaviors after magnetic field annealing. For pure $BiFeO_3$ samples, the remnant polarizations (P_r) are suppressed; in contrast, for $Bi_{0.85}Dy_{0.15}FeO_3$ samples, P_r is greatly enhanced. Possible mechanisms for the effects of magnetic field annealing have been discussed.

1. Introduction

$BiFeO_3$ (BFO), because of its ferroelectric and antiferromagnetic ordering well above room temperature (RT), has attracted considerable scientific interests as a popular multiferroic material [1,2]. The coexistence of the dual order parameters in BFO can give rise to a possible magnetoelectric effect, and thus the material may have promising applications in future innovative electronic devices [3,4]. However, in spite of the RT multiferroicity, it is hard to obtain a desired sample owing to the main drawbacks of poor magnetization and low electrical resistivity [5,6]. In the recent years, many promising methods have been adapted for one thing to overcome these challenges, and for another to achieve an exhaustive comprehension of the material [2,7–9]. Hence, the development of novel fabrication methods is necessary for further understanding the performances of BFO and BFO-based materials.

It has been known that the microstructure and magnetic properties of some magnetic materials can be strongly influenced by growth in high magnetic fields due to the orientation effect [10]. Meanwhile, a variety of phase transitions can be induced using an applied magnetic field [11,12]. Furthermore, a permanent magnetic anisotropy may be developed in certain alloys after magnetic annealing [13]. These induced morphology, structure, and even property evolutions evoke considerable interest to study the basic physical phenomenon and design typical materials for applications. So a magnetic field provides an important approach in the process of many advanced materials. Yet, there have been few literatures to report the effects of magnetic annealing on BFO-based materials. Therefore, in this study, the magnetic annealing experiments have been carried out by sintering the precursor powder of pure BFO and $Bi_{0.85}Dy_{0.15}FeO_3$ (BDF) in magnetic fields of 0, 5, and 10 T to study the influences of the magnetic annealing on the crystalline structures and the multiferroic behaviors.

2. Experimental procedures

The precursor powders of BFO and BDF were prepared by a sol–gel auto-combustion method. Typically, the precursor powders of BFO were prepared using analytical reagent grade bismuth nitrate [$Bi(NO_3)_3 \cdot 5H_2O$], and ferric nitrate [$Fe(NO_3)_3 \cdot 9H_2O$] as starting materials. Firstly, the above metal nitrates in mole ratio of 1:1 together with certain amount of nitric acid were dissolved in a required amount of distilled water. Then, glycine was added as a fuel. Subsequently, the resulting homogeneous solution was put into a 1000 W microwave oven for auto-combustion experiments to produce voluminous powders. The obtained powders were pressed into disk samples and treated by magnetic annealing at 780 °C for 30 min. For BDF, stoichiometric amount of Dy_2O_3 was dissolved in certain amount of diluted nitric acid in the

* Corresponding author.
E-mail address: ywma@mail.iee.ac.cn (Y. Ma).
[1] Both contribute equally.

0304-8853/$ - see front matter © 2012 Elsevier B.V. All rights reserved.
doi:10.1016/j.jmmm.2012.02.030

beginning. Then bismuth nitrate and ferric nitrate in a proper mole ratio were also dissolved in the solution above. The following processes were similar to those of BFO samples. Here we denoted the samples as BFO (0, 5, or 10 T) and BDF (0, 5, or 10 T) according to various applied magnetic fields.

The magnetic annealing procedure was conducted as described below. Initially, a magnetic field (0, 5, or 10 T) was applied after the samples were put into the furnace; next the furnace was heated up to 780 °C followed by holding for 30 min; at last the external magnetic field was not removed until the furnace was cooled to RT.

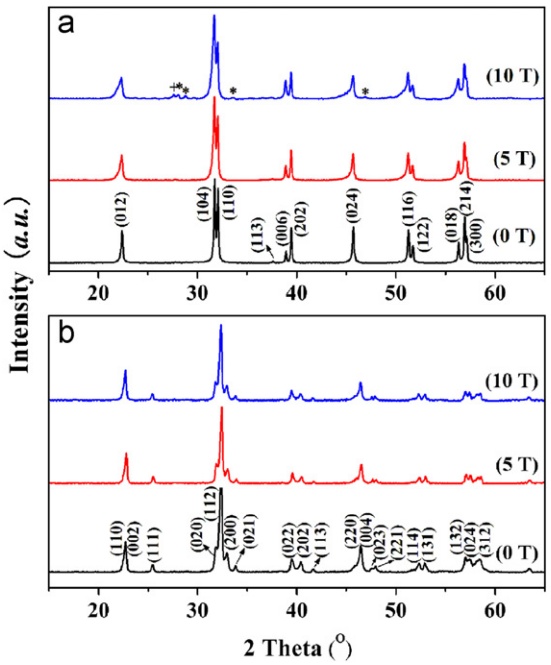

Fig. 1. X-ray diffraction patterns of BFO and BDF samples. (a) BFO 0, 5, and 10 T. (b) BDF 0, 5, and 10 T. (∗ and + indicate peaks due to $Bi_2Fe_4O_9$ and possible $Bi_{25}FeO_{39}$ phases, respectively).

The crystal structure identification was performed by an X-ray diffraction (XRD) machine with Cu $K\alpha$ radiation. The microstructure analysis was conducted using Scanning Electron Microscopy (SEM). Raman spectra were measured in the backscattering geometry using a confocal micro-Raman spectrometer (Jobin Yvon HR800) with the 532 nm laser line as the excitation source. The magnetic measurements were performed on a Physical Property Measurement System. The ferroelectric properties were measured on an aixACCT TF Analyzer 2000 System. Dielectric properties were obtained using an impedance analyzer (HP 4294A). All the measurements were carried out at RT.

3. Results and discussion

Fig. 1(a) and (b) shows the XRD patterns of BFO and BDF samples, respectively, annealed under different magnetic fields. The XRD patterns of BFO (0, 5 T) samples can be indexed to a rhombohedral distortion perovskite structure with a space group of *R*3*c*. No observable impurity peaks were detected for the sample annealed at 0 T field. However, for the 10 T-annealed sample, extra peaks from the impurity phase of $Bi_2Fe_4O_9$ and $Bi_{25}FeO_{39}$ [marked with "∗" and "$^+$" in Fig. 1(a) 10 T, respectively] can be observed. In addition, it is clear that all diffraction peaks are broadened after magnetic field annealing. In contrast to the rhombohedral *R*3*c* structure observed in BFO, a dominant orthorhombic $LnFeO_3$-like structure (space group *Pnma*) was found in BDF samples, as shown in Fig. 1(b), 0 T. A detailed analysis about phase transitions caused by dysprosium substitution can be found in previous reports [14,15]. Furthermore, broadened diffraction peaks or secondary phases are not observed in the BDF samples after the magnetic field annealing, as shown in Fig. 1(b). It is evident that the magnetic annealing has no influence on the crystal structure of BDF samples in this study.

Fig. 2(a), (b) and (c) shows the representative SEM images taken from the fresh fracture surface of pure BFO 0, 5, and 10 T samples, respectively. Uniform surface morphology with a narrow grain size distribution is observed in these samples. The grain size is of several microns. Moreover, magnetic field annealing has little influence on morphology and crystallite sizes, implying that the

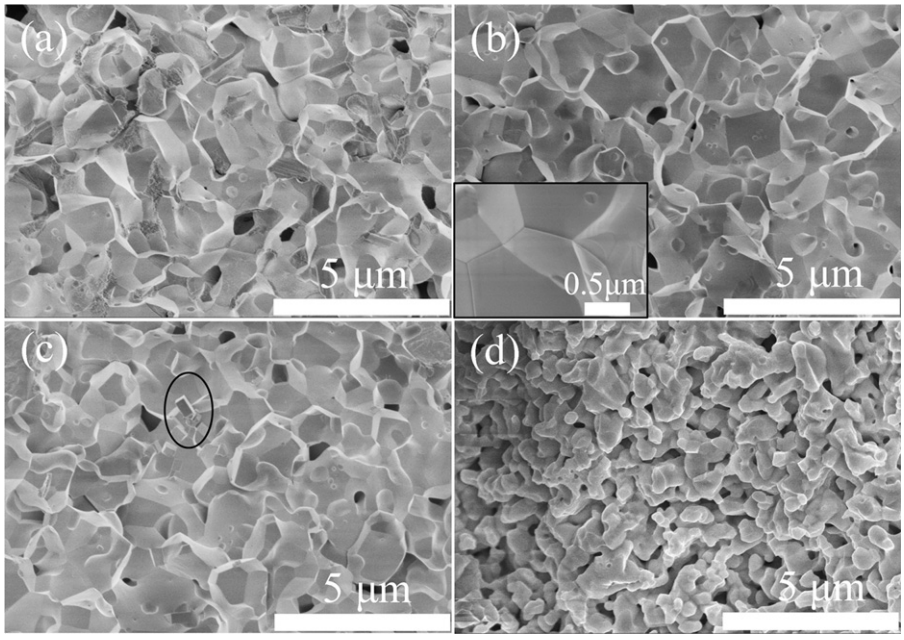

Fig. 2. SEM images of (a) BFO (0 T), (b) BFO (5 T), (c) BFO (10 T) and (d) BDF (0 T). The inset in (b) shows a high magnification image of BFO (5 T).